

Pathogenic variants in the NLRP3 LRR domain at position 861 are responsible for a boost-dependent atypical CAPS phenotype.

Antoine Fayand^{1,2,*} MD, Margaux Cescato^{2,*} M.Sc, Laurent Le Corre² Ph.D, Alexandre Terré^{1,3} MD, Margaux Wacheux² M.Sc, Yixiang YJ Zhu² M.Sc, Armelle Melet² Ph.D, Thomas RJ Moreau^{2,4} M.Sc, Bahram Bodaghi⁵ MD, Fabrice Bonnet⁶ MD, Didier Bronnimann⁶ MD, Laurence Cuisset⁷ MD, Raquel Faria⁸ MD, Gilles Grateau¹ MD, Ph.D, Pascal Pillet⁹ MD, Catharina M Mulders-Manders¹⁰ MD, Benedicte Neven¹¹ MD, Ph.D, Pierre Quartier^{11,12} MD, Ph.D, Olivier Richer⁹ MD, Léa Savey¹ MD, Marie-Elise Truchetet¹³ MD, Bénédicte F Py¹⁴ Ph.D, Guilaine Boursier¹⁵ MD, Ph.D, Jean-Philippe Herbeuval² Ph.D, Sophie Georgin-Lavialle^{1,&, †} MD, Ph.D, Mathieu P Rodero^{2,& †} Ph.D.

12

¹ Sorbonne Université, department of internal medicine, National reference center for autoinflammatory diseases and AA amyloidosis, Tenon Hospital, APHP, Paris, France.

² Université Paris Cité, CNRS, Laboratoire de Chimie et de Biochimie Pharmacologiques et Toxicologiques, F-75006 Paris, France

³ Université Paris Cité, Inserm, Institut Imagine, Laboratoire Mécanismes cellulaires et moléculaires des désordres hématologiques et implications thérapeutiques, F-75015 Paris, France

⁴ Translational Immunology Unit, Institut Pasteur, Université Paris Cité, Paris, France.

⁵ Sorbonne Université, department of Ophthalmology, IHU FOReSIGHT, Pitié-Salpêtrière Hospital, APHP, Paris, France

⁶ CHU de Bordeaux, Hôpital Saint-André, Service de Médecine Interne et Maladies Infectieuses, Bordeaux, France

⁷ Université de Paris Cité, Assistance Publique Hôpitaux de Paris, Hôpital Cochin, Paris, France

⁸ Unidade de Imunologia Clínica - Centro Hospitalar Universitário do Porto; UMIB - Unit for Multidisciplinary Research in Biomedicine, ICBAS - School of Medicine and Biomedical Sciences, University of Porto; ITR - Laboratory for Integrative and Translational Research in Population Health, Porto, Portugal.

⁹ Service de pédiatrie et rhumatologie pédiatrique, Hôpital Pellegrin-enfants, Bordeaux

¹⁰ Department of Internal Medicine, Radboud expertise center for immunodeficiency and autoinflammation, Radboud University Medical Center, Nijmegen, The Netherlands.

¹¹ Université de Paris Cité, Pediatric Immunology-Hematology and Rheumatology Unit, Necker hospital, Paris, France.

¹² RAISE reference centre for rare diseases

37 ¹³ Department of Rheumatology, Hopital Pellegrin and UMR5164 ImmunoConcept, Bordeaux
38 University, Bordeaux University Hospital, Bordeaux, France.

39 ¹⁴ CIRI, Centre International de Recherche en Infectiologie, Univ Lyon, Inserm, U1111,
40 Université Claude Bernard Lyon 1, CNRS, UMR5308, ENS de Lyon, F-69007, Lyon, France.

41 ¹⁵ Laboratoire de Génétique des Maladies rares et autoinflammatoires, Service de Génétique
42 moléculaire et cytogénomique, National reference center for autoinflammatory diseases and
43 AA amyloidosis, CHU Montpellier, Univ Montpellier, Montpellier, France

44

45 * Contributed equally

46 & Codirected the study

47

48 † Corresponding authors: Mathieu Rodero, UMR8601, 45 rue des St Pères 75006 Paris.
49 mathieu.rodero@u-paris.fr and Sophie Georgin-Lavialle: Sorbonne Université, APHP, Tenon
50 hospital, Department of Internal Medicine, National reference center for autoinflammatory
51 diseases and inflammatory amyloidosis (CEREMAIA), Paris, France. [sophie.georgin-](mailto:sophie.georgin-lavialle@aphp.fr)
52 lavialle@aphp.fr

53

54 **Conflict of interest**

55 All the authors declare that they have no relevant conflicts of interest.

56

57

58 **Abstract**

59

- 60 • **Background:** Cryopyrin-associated periodic syndrome (CAPS) is associated with
61 *NLRP3* pathogenic variants, mostly located in the NACHT domain. Cold induced
62 urticarial rash is one of the main clinical features. We however identified a series of 14
63 patients with pathogenic variants of the Y861 residue (p.Tyr861) of the LRR domain of
64 *NLRP3* and minimal prevalence of cold-induced urticarial rash.
- 65 • **Objective:** We aimed to address a possible genotype / phenotype correlation for CAPS
66 patients and to investigate at the cellular levels the impact of the Y861C substitution
67 (p.Tyr861Cys) on *NLRP3* activation.
- 68 • **Methods:** Clinical features of 14 CAPS patients with heterozygous substitution at
69 position 861 in the LRR domain of *NLRP3* were compared to clinical features of 48
70 CAPS patients with pathogenic variants outside the LRR domain of *NLRP3*. IL-1 β
71 secretion by PBMCs and purified monocytes from patients and healthy donors was
72 evaluated following LPS and MSU stimulation.
- 73 • **Results:** Patients with substitution at position 861 of *NLRP3* demonstrated a higher
74 prevalence of sensorineural hearing loss while being less prone to skin urticarial. In
75 contrast to classical CAPS patients, cells from patients with a pathogenic variant at
76 position 861 required an activation signal to secrete IL-1 β but produced more IL-1 β
77 during the early and late phase of secretion than cells from healthy donors.
- 78 • **Conclusion:** Pathogenic variants of Y861 of *NLRP3* drive a boost-dependent over
79 secretion of IL-1 β associated with an atypical CAPS phenotype.

80

81 **Clinical Implications**

82 *NLRP3* pathogenic variants should be considered as a possible cause of early onset hearing loss
83 in patients with elevated inflammatory biomarkers, even in the absence of skin urticarial rashes.

84

85 **Capsule Summary**

86 Pathogenic variants of the residue 861 of *NLRP3* drive an atypical CAPS phenotype associated
87 with increased prevalence of hearing loss but less frequent skin urticaria compared to typical
88 CAPS.

89

90 **Key Words**

91 *NLRP3*, CAPS, inflammasome, LRR domain, Interleukin-1, hear loss, deafness, urticaria

92

93

94

95

96 **Abbreviations**

- 97 ASC: Apoptosis-associated speck-like protein containing a CARD domain
- 98 ATP: adenosine triphosphate
- 99 CAPS: cryopyrin-associated periodic syndrome
- 100 CD14: Cluster of differentiation 14
- 101 CRP: C-reactive protein
- 102 cryoEM: cryogenic electron microscopy
- 103 ELISA: enzyme-linked immunosorbent assay
- 104 FMF: Familial Mediterranean fever
- 105 HC: healthy control
- 106 LPS: lipopolysaccharide
- 107 MD: Molecular Dynamics
- 108 NACHT: NAIP (neuronal apoptosis inhibitor protein), C2TA (MHC class 2 transcription
109 activator), HET-E (incompatibility locus protein from *Podospora anserina*), TP1 (telomerase-
110 associated protein)
- 111 NEK7: NIMA Related Kinase 7
- 112 NLRP3: NOD-like receptor family, pyrin domain containing 3
- 113 PBMC: Peripheral blood mononuclear cell
- 114 PRR: Pattern recognition receptors
- 115 RPMI: Roswell Park Memorial Institute medium
- 116 SEM: standard error of the mean
- 117 SD: standard deviation
- 118 TSM1: target of methylation-induced silencing
- 119 LRR: Leucine-Rich Repeat
- 120 IL-1 β : interleukine 1 beta
- 121 IL-18: interleukine 18
- 122 MSU: monosodium urate crystals
- 123 WT: Wild-Type
- 124
- 125

126 **Introduction:**

127 NOD-like receptor family, pyrin domain containing 3 (NLRP3) protein is probably the most
128 studied pattern recognition receptors (PRRs), that assemble inflammasome complex upon
129 activation (1). The full canonical activation of the NLRP3 inflammasome is dependent on a two
130 steps process (2). The first step, named “priming”, controls the transcriptional upregulation of
131 NLRP3 and the inflammasome substrates pro-IL-1 β , pro-IL-18 , as well as license NLRP3 for
132 later activation through post-translational modifications including phosphorylations (3,4) and
133 deubiquitinations (5) linked to structural changes and subcellular relocalisation. The second
134 step, named “activation” initiates the final conformation change of NLRP3 protomers. During
135 the priming/activation process NLRP3 transient from an inactive ADP-bound 10-12mers
136 NLRP3 “cage” structure to an active ATP-bound pentamers inflammasome (6–9) leading to
137 caspase-1 activation, and therefore the maturation and release of IL-1 β and IL-18 as well as
138 pyroptotic inflammatory cell death. Heterozygous missense gain of function variants in *NLRP3*
139 have been associated with an autoinflammatory syndrome called cryopyrin-associated periodic
140 syndrome (CAPS) (10). Besides systemic inflammation, intermittent fever and arthralgia,
141 CAPS patients display very specific features including pseudo-urticarial rash often triggered by
142 exposure to cold, neuroinflammatory features such as aseptic meningitidis, sensorineural
143 hearing loss, various ocular manifestations like conjunctivitis and uveitis, and less frequently
144 oral aphthous and digestive features(11). Interestingly, *NLRP3* pathogenic variants found among
145 CAPS patients are almost exclusively located in the NACHT domain of NLRP3. These
146 mutations are thought to impact ATPase activity or key subdomain interaction surface that
147 intervene in the final opening of the inflammasome structure (8,9) As a result, priming step
148 alone is sufficient to drive significant IL-1 β production and this *in vitro* dysregulation profile is
149 therefore considered as a signature of CAPS (12). The most effective treatment for CAPS
150 patients are IL-1 β inhibitors (13)(14).

151

152

153

154

155

156

157 **Methods**

158 **Human sample collection.**

159 The blood from healthy donors was obtained from “*Etablissement Français du Sang*”
160 (convention # 07/CABANEL/106), Paris, France. For CAPS patients’ blood, the study was
161 approved by the Comité de Protection des Personnes (N° EudraCT: 2018-A01358-47) in
162 France. Experimental procedures with human samples were done according to the European
163 Union guidelines and the Declaration of Helsinki. Clinical data were extracted from the JIR
164 (Juvenile Inflammatory Rheumatism)- cohort; an international multicenter data repository
165 established by the National Commission on Informatics and Liberty (CNIL; authorization
166 number N°: 914677). Patients consented to be included in the JIR-cohort and were informed
167 that data collected in medical records might be used for research studies in accordance with
168 privacy rules.

169

170 **Culture conditions**

171 *In vitro* experiments were performed using frozen human mononuclear cells from peripheral
172 blood isolated by centrifugation in density gradient medium (STEMCELL Technologies).
173 Human monocytes were purified by positive selection with Human CD14 microbeads
174 (Miltenyi). Peripheral blood mononuclear cells (PBMC) and monocytes were cultured in RPMI
175 1640 (Invitrogen, Gaithersburg, MD) (R10) containing 10% heat-inactivated fetal bovine
176 serum.

177

178 **Measurement of ASC protein aggregates in serum**

179 Sera ASC aggregates were determined using an adapted previously described method adapted
180 for our purposes (24). One hundred microliters of patients or HC serum were incubated with
181 2.5 μ L of phycoerythrin anti-ASC (TMS-1) antibody (Biolegend) for 1 hour at room
182 temperature. Analyses were performed on the BD LSRFortessa™ X-20 flow cytometer
183 instrument (BD Biosciences). Nonfluorescent 1- μ m microspheres (Thermo Fisher Scientific)
184 were used as a guide to gate around ASC specks. Total events in the gated area were divided
185 by 100 for the evaluation of ASC speck per microliter.

186

187 IL-1 β and IL-18 detection by ELISA

188 PBMCs were seeded at $1 \cdot 10^6$ cells /mL and monocytes isolated from PBMCs at $1 \cdot 10^5$ cells /mL.
189 Standard protocol consists in a priming with LPS 10ng/ml. After 3h PBMC were activated with
190 MSU (monosodium urate crystals) 200 μ g/ml. After 3 hours the media were collected and
191 analyzed by ELISA. For kinetic experiments, the media were collected 30 minutes, 1 hour, 2
192 hours, 3 hours and 6 hours after MSU. For basal production on unstimulated cells, PBMC or
193 purified monocytes were cultured overnight. IL-1 β and IL18 were measured in cell supernatant
194 and/or patient's plasma using a kit from R&D (DY201-05 and DY318-05 respectively)
195 according to supplier recommendations.

196

197 Legendplex:

198 Cytokines in patients' plasma were quantified using bead-based multiplex assays
199 (LEGENDplex 13-plex HU Essential Immune Response Panel). The experiment was conducted
200 according to the manufacturer protocol. Briefly, diluted plasma were incubated with Capture
201 Beads for 2h. Following centrifugation, supernatants were discarded and biotinylated detection
202 antibodies were added for 1h. After incubation with SA-PE, supernatants are discarded and
203 samples are resuspended in the provided wash buffer to read on the flow cytometer.

204

205 In silico Modeling:

206 All *in silico* studies were performed within the Biovia Discovery Studio (DS 2022) suite.
207 Mutants models were generated using the cryo-EM structure of the wt NLRP3 in complex with
208 NEK7 (PDB: 6NPY) and the Modeller program (Version: 9.24) implemented in the Building
209 Mutant protocol of DS. Short Molecular Dynamics MD simulations (5 ns) were run using the
210 NAMD program (25) implemented in DS and the CHARMM36m force field. The average
211 interfacial interaction energy between NLRP3 and NEK7, based on the sum of the van der
212 Waals and electrostatic interactions was calculated on the last ns of the 5ns MD simulations
213 using the Calculate Interaction Energy tool of DS- Analysis of the NLRP3/NEK7 interactions
214 was conducted with the Analysis Protein Interface tool.

215

216 Statistics

217 All statistical analyses were performed using GraphPad Prism (version 9.1.1). Data on the
218 figures are presented as mean (\pm SD for the kinetic experiments). For experimental data,
219 statistical analysis were performed either using non-parametric One-way ANOVA followed by
220 Kruskal-Wallis multiple comparison test or non-parametric 2-tailed Mann-Whitney test (IL-18
221 plasma assay). For clinical information, non-categorical data were analyzed using Mann
222 Whitney test and categorical data using Fisher test. P values less than 0.05 were considered
223 significant.

224

225 **Results**

226 **Pathogenic variants of the residue 861 in NLRP3 drive an atypical CAPS disease.**

227 Nine patients carrying a heterozygous Y861C missense variant (NM_004895.5 : c.2582A>G
228 p.(Tyr861Cys)) of *NLRP3*, and 5 carrying a heterozygous Y861H variant (NM_004895.5 :
229 c.2581T>C p.(Tyr861His)) were included in France, Holland, and Portugal (15,16). Depending
230 on the first methionine used for numbering, these variants are also known as c.2576A>G
231 p.(Tyr859Cys) and c.2575T>C p.(Tyr859His) using NM_001243133.2. These variants are
232 respectively reported pathogenic and likely pathogenic in the ClinVar database.

233 Unlike most CAPS causing pathogenic variants that are located in the NACHT domain, these
234 substitutions involve a tyrosine residue in the LRR domain of NLRP3 (**Figure 1A**). All patients
235 belonged to large families with dominant transmission of the mutation (**Figure 2**).

236 While these patients display typical features of CAPS as ophthalmological manifestations such
237 as recurrent conjunctivitis, uveitis or papillary edema (93%), arthromyalgia (79%) and aseptic
238 meningitidis (43%) (**Figure 1 B, C, D and E**), some other main features are significantly
239 differentially observed compared to our cohort of 48 CAPS patients with pathogenic variants
240 outside of the LRR domain. Indeed, they have more sensorineural hearing loss (100% Vs 63%,
241 $p=0.006$), more headaches (86% Vs 45%, $p=0.013$), less urticarial rash (29% Vs 94%, $p<0.001$)
242 and less aphtosis (7% Vs 53%, $p=0.004$). Of note, 3 patients from a same family had
243 hypereosinophilia, a feature not found in our typical CAPS cohort (21% Vs 0%, $p=0.037$) (**table**
244 **I and sup table I**).

245 In order to confirm that the patients with substitution of the tyrosine residue at position 861 of
246 NLRP3 were affected by an inflammasomopathy we quantified ASC speck and IL-18 in their
247 plasma. ASC speck concentration in plasma of NLRP3^{Y861C} patients was higher than in healthy
248 donors and comparable to the levels observed in typical CAPS patients or patients with FMF

249 **(Figure 1 F)**. Similarly, IL-18 concentration was significantly higher in NLRP3^{Y861C} patients
250 compared to controls (mean: 216,4 pg/ml \pm 9,1 pg/ml and 84,1 pg/ml \pm 4,1 pg/ml respectively;
251 $p=0,0023$ – Two-tail Mann-Whitney test) **(Figure 1 G)**. No other cytokine were found to be
252 significantly over express in typical CAPS or NLRP3^{Y861C} patients (Sup Fig1).

253 Finally, in line with these results and what is known in classical CAPS, IL-1 β inhibitors were
254 very efficient in all patients. Most clinical symptoms quickly resolved, with marked
255 improvement in general condition and almost complete resolution of headache, ophthalmic
256 manifestations and arthralgia. Additionally, hearing ceased to deteriorate. Accordingly,
257 biological response was immediate, with normalization of CRP, SAA and blood count within
258 8 days.

259

260 **Activation signal is required to fully activate inflammasome in cells from NLRP3^{Y861C}** 261 **patients.**

262 To date, the only characterisation of primary immune cells from NLRP3^{Y861C} mutated patients
263 suggests that patients' PBMCs spontaneously produced IL-1 β , in the absence of any stimulus,
264 either prime and/or boost signal (15). However, in our hands, neither PBMC nor isolated
265 monocytes from NLRP3^{Y861C} produced IL-1 β in the absence of a priming or activating signal
266 **(Figure 3A and B)**. Thus, we tested the response of NLRP3^{Y861C} mutated cells to priming signal
267 only. As for cells from healthy donors, priming with LPS alone induced a very slight production
268 of IL1- β in NLRP3^{Y861C} mutated PBMCs and monocytes while NLRP3 NACHT domain
269 mutated cells were producing higher quantities ($2,4 \pm 0,48$ fold HD, $p > 0,999$ and $21,7 \pm 0,99$
270 fold HD, $p = 0,0050$ respectively for PBMC, One-way ANOVA, Kruskal-Wallis test) **(Figure**
271 **3C and D)**. These results strongly suggest that NLRP3^{Y861C} patients have a distinct
272 pathophysiological mechanism compared to the more common CAPS driving NACHT
273 pathogenic variants of NLRP3. Finally, the comparison of IL1 β production after prime plus
274 boost stimulation in cells from healthy donors, NLRP3^{Y861C} mutated patients and typical CAPS
275 patients returned comparable levels **(Figure 3C and D)**. Overall, despite compelling clinical
276 and genetic evidence that NLRP3^{Y861C} drives an atypical CAPS phenotype in most patients, our
277 in vitro results could not differentiate NLRP3 activation between healthy donors and
278 NLRP3^{Y861C} mutated patients.

279

280 **Cells from NLRP3^{Y861C} patients demonstrate sustained IL-1 β production compared to**
281 **cells from healthy donors.**

282 Recently, *Caseley et al* reported a patient with a NLRP3^{R920D} substitution in the LRR domain
283 of NLRP3 resulting in an atypical inflammatory syndrome (17). Based on modelling studies,
284 the authors suggested that the mutation enhanced the electrostatic complementarity between the
285 LRR portion of NLRP3 and NEK7 leading to an increased binding affinity between the two
286 partners. Since Y861 is located at the interface of NLRP3 and NEK7 (**Figure 4A**), we
287 hypothesized that Y861 pathogenic variants might potentially enhance the NLRP3/NEK7
288 binding as well.

289 To evaluate the impact of the Y861C and Y861H substitution on the stability of the interaction
290 between NLRP3 and NEK7, we performed short Molecular Dynamics (MD) simulations
291 starting from the cryoEM structure of the NLRP3/NEK7 complex (PDB:6NPY, (18)). We
292 examined the binding interface of C861 and H861 mutant models and calculated the interaction
293 energy for each NLRP3/NEK7 complex. A model of the R920Q mutation was also generated
294 for the sake of comparison. Our results with R920Q model are in agreement with those
295 previously reported by *Caseley et al* (17). R920Q mutation resulted in an enhanced binding
296 between NLRP3 and NEK7 (**Figure 4A**). Compared to WT, Y861C model had a positive effect
297 on stability between NLRP3 and NEK however the Y861H mutation proved to be detrimental
298 to the stability of the NLRP3/NEK interface. Thus, given the phenotypic similarities between
299 Y861C and Y861H patients, increased binding affinity between NLRP3 and NEK7 probably
300 does not explain the atypical phenotypes observed in most of these patients. This might also be
301 supported by the strong phenotypic difference between the NLRP3 R920Q mutated patient and
302 NLRP3 Y861C, and Y861H patients.

303 Previous work in mice and human derived monocytic cell lines (19) suggest that the Y861
304 residue (Y859 in mice) is central for the control of NLRP3 activation. It is proposed that
305 phosphorylation of Y861 promotes the addressing of activated NLRP3 to phagolysosome
306 leading to a reduction of the NLRP3 pool available for inflammasome assembly (20). We
307 anticipate that such mechanism should results in increased early production of IL-1 β by
308 patient's cells. In order to test this hypothesis, we performed a kinetic of IL-1 β production
309 following LPS and MSU stimulation on isolated monocytes from healthy donors and 3
310 NLRP3^{T861C} mutated patients. Our results highlight a strongest production of IL1 β during the
311 first two hours post boost in monocytes from the 3 NLRP3^{T861C} mutated patients compared to
312 healthy donors supporting our hypothesis (**Figure 4B**). We also observed a sustained

313

314 production of IL1 β in monocytes from patients. Indeed, while the secretion stopped after 3
315 hours in cells from most healthy donors, we could still observe a production of IL-1 β between
316 3 and 6 hours post boost in the monocytes from the 3 tested NLRP3^{T861C} mutated individuals
317 **(Figure 4C)**. These latest results also support the hypothesis of a defective deactivation of the
318 inflammasome complex.

319 **Discussion**

320 Altogether, we describe 14 patients with pathogenic variants located in the LRR domain of
321 NLRP3 at position 861. This series highlights a clear genotypes /phenotypes correlation with
322 all patients displaying hearing loss, and 10 out of 14 devoid of pseudo-urticarial rash **(Figure**
323 **5)**. This remarkable difference in phenotype observed in patients with pathogenic variants
324 outside the LRR domain (21) might be explained by the distinct activation profile of NLRP3
325 depending on the localization of the disease-causing variants. Indeed, in contrast to cells from
326 typical CAPS, PBMCs and monocytes from NLRP3^{T861C} mutated patients required a boost
327 signal for full inflammasome activation. However, patients' cells demonstrated exacerbated
328 early IL1 β secretion and sustained IL1 β secretion following "prime and boost" activation when
329 compared to healthy donors. It remains unclear what causes this exacerbated response to
330 stimuli. Previous studies in mice suggest that phosphorylation of the Y859 residue promote
331 NLRP3 degradation (19). In their models, defective phosphorylation of Y859 is associated with
332 defective addressing of activated NLRP3 to phagolysosomes (20). Nevertheless, another study
333 performed using human NLRP3 expressed in mice cells suggests that it is not the
334 phosphorylation of Y861, but the phosphorylation of Y918 that control NLRP3 activity (22).
335 Further experiments will be needed on human cells to confirm or exclude the contribution of
336 Y861 to NLRP3 degradation. Another nonexclusive hypothesis is that the modification of the
337 electrostatic charge of NLRP3 LRR domain caused by the Y861C substitution either stabilizes
338 the active inflammasome complex or destabilizes the inactive cage conformation. Indeed,
339 charges in the LRR concave side plays a major role in NEK7 recruitment to NLRP3 to form the
340 inflammasome and Y861C may drives an increase affinity of NLRP3 for NEK7, thus resulting
341 in an overactivated inflammasome. A similar mechanism was already reported for a R920Q
342 substitution causing an atypical auto inflammatory disease (17). Further experimental
343 approaches are needed to fully understand how these mutation impact NLRP3 function and
344 regulation and contribute to the CAPS phenotypes. Of note, we observed a non-statistically
345 significant trend towards an overall increase IL-1 β secretion in cells from Y861C patients

346 compare to cells from healthy donors upon LPS + MSU treatment. Future experiment on a
347 larger group of patients and control should help to determine if this observation is due to inter-
348 individual variability or is a hallmark of this mutation.

349 The low prevalence of skin manifestation and aphthosis associated to the high prevalence of
350 deafness and headaches in NLRP3^{Y861C} and NLRP3^{Y861H} mutated patients might be explained
351 by the distinct pathophysiological mechanism compared to typical CAPS. Skin pseudo-
352 urticarial rash seen in most CAPS could result from a local production of IL-1 β triggered by an
353 uncontrolled priming signal in patients with mutation leading to activation signal independent
354 NLRP3 inflammasome formation (*ie* mutation in the NACHT domain). Conversely, the
355 preserved dependence on the boost of Y861 pathogenic variants could protect these patients
356 from the cutaneous phenotype of CAPS. On the other hand, NLRP3^{Y861C} and NLRP3^{Y861H}

357

358 mutated patients show high prevalence of sensorineural hearing loss which is reminiscent of
359 what was observed in two families with a NLRP3^{R920D} mutation which is in the close vicinity
360 of Y861 (23). Better understanding of the impact of these variants on local and systemic
361 inflammation in humans might help to explain these phenotypic specificities.

362

363 In conclusion, it appears that the differential diagnosis of a dominantly inherited sensorial
364 hearing loss should include cryopyrinopathy in individuals with elevated CRP, even in the
365 absence of urticaria. This is particularly true in patients with ophthalmological (conjunctivitis)
366 and neurological (headache) features and hypereosinophilia. A genetic sequencing looking for
367 *NLRP3* pathogenic variants by next generation sequencing could reduce the diagnostic delay
368 and prevent the risks of hearing or visual sequelae and AA amyloidosis.

369

370 **Acknowledgments**

371 We thank all the affected patients and their family, and the healthy individuals used as controls.
372 We thank the Macromolecular Modeling Platform of UMR8601, Université de Paris Cité for it
373 help with modelling, Agence Régionale de Santé Île-de-France and hôpitaux universitaires de
374 Strasbourg for supporting the project with the “bourse année-recherche” educational grant and
375 “la Fondation pour la Recherche Médicale” for providing the Ph.D scholarship of Margaux
376 Cescato. We thank Irina Giurgea for her help with several French patients genotyping.

377

378 **Funders**

379 SGL: ANR INFLAMAST AAPG 2017 CE17 and foundation APHP.

380 MPR was supported by the Agence National de la Recherche: ANR-21-CE17-0025 JDMINF2.

381

382 **Data Availability**

383 The datasets generated during and/or analysed during the current study are available from the
384 corresponding author on reasonable request.

385 **Bibliography**

- 386 1. Swanson KV, Deng M, Ting JP-Y. The NLRP3 inflammasome: molecular activation and
387 regulation to therapeutics. *Nat Rev Immunol*. 2019 Aug;19(8):477–489.
- 388 2. He Y, Hara H, Núñez G. Mechanism and regulation of NLRP3 inflammasome activation.
389 *Trends Biochem Sci*. 2016 Dec;41(12):1012–1021.
- 390 3. Song N, Liu Z-S, Xue W, Bai Z-F, Wang Q-Y, Dai J, et al. NLRP3 phosphorylation is an
391 essential priming event for inflammasome activation. *Mol Cell*. 2017 Oct 5;68(1):185–
392 197.e6.
- 393 4. Niu T, De Rosny C, Chautard S, Rey A, Patoli D, Gros Lambert M, et al. NLRP3
394 phosphorylation in its LRR domain critically regulates inflammasome assembly. *Nat*
395 *Commun*. 2021 Oct 6;12(1):5862.
- 396 5. Juliana C, Fernandes-Alnemri T, Kang S, Farias A, Qin F, Alnemri ES. Non-
397 transcriptional priming and deubiquitination regulate NLRP3 inflammasome activation. *J*
398 *Biol Chem*. 2012 Oct 19;287(43):36617–36622.
- 399 6. Fletcher DJ. Coping with insomnia. Helping patients manage sleeplessness without drugs.
400 *Postgrad Med*. 1986 Feb 1;79(2):265–274.
- 401 7. Andreeva L, David L, Rawson S, Shen C, Pasricha T, Pelegrin P, et al. NLRP3 cages
402 revealed by full-length mouse NLRP3 structure control pathway activation. *Cell*. 2021 Dec
403 22;184(26):6299–6312.e22.
- 404 8. Brinkschulte R, Fußhöller DM, Hoss F, Rodríguez-Alcázar JF, Lauterbach MA, Kolbe C-
405 C, et al. ATP-binding and hydrolysis of human NLRP3. *Commun Biol*. 2022 Nov
406 3;5(1):1176.
- 407 9. Xiao L, Magupalli VG, Wu H. Cryo-EM structures of the active NLRP3 inflammasome
408 disc. *Nature*. 2022 Nov 28;
- 409 10. Hoffman HM, Mueller JL, Broide DH, Wanderer AA, Kolodner RD. Mutation of a new
410 gene encoding a putative pyrin-like protein causes familial cold autoinflammatory
411 syndrome and Muckle-Wells syndrome. *Nat Genet*. 2001 Nov;29(3):301–305.
- 412 11. Quartier P, Rodrigues F, Georgin-Lavialle S. [Cryopyrin-associated periodic syndromes].
413 *Rev Med Interne*. 2018 Apr;39(4):287–296.
- 414 12. Agostini L, Martinon F, Burns K, McDermott MF, Hawkins PN, Tschopp J. NALP3 forms
415 an IL-1beta-processing inflammasome with increased activity in Muckle-Wells
416 autoinflammatory disorder. *Immunity*. 2004 Mar;20(3):319–325.
- 417 13. Hawkins PN, Lachmann HJ, Aganna E, McDermott MF. Spectrum of clinical features in
418 Muckle-Wells syndrome and response to anakinra. *Arthritis Rheum*. 2004 Feb;50(2):607–
419 612.
- 420 14. Hoffman HM, Rosengren S, Boyle DL, Cho JY, Nayar J, Mueller JL, et al. Prevention of
421 cold-associated acute inflammation in familial cold autoinflammatory syndrome by
422 interleukin-1 receptor antagonist. *Lancet*. 2004 Nov 19;364(9447):1779–1785.
- 423 15. Jéru I, Marlin S, Le Borgne G, Cochet E, Normand S, Duquesnoy P, et al. Functional
424 consequences of a germline mutation in the leucine-rich repeat domain of NLRP3
425 identified in an atypical autoinflammatory disorder. *Arthritis Rheum*. 2010
426 Apr;62(4):1176–1185.

- 427 16. Mulders-Manders CM, Kanters TA, van Daele PLA, Hoppenreijns E, Legger GE, van Laar
428 JAM, et al. Decreased quality of life and societal impact of cryopyrin-associated periodic
429 syndrome treated with canakinumab: a questionnaire based cohort study. *Orphanet J*
430 *Rare Dis.* 2018 Apr 20;13(1):59.
- 431 17. Caseley EA, Lara-Reyna S, Poulter JA, Topping J, Carter C, Nadat F, et al. An atypical
432 autoinflammatory disease due to an LRR domain NLRP3 mutation enhancing binding to
433 NEK7. *J Clin Immunol.* 2022 Jan;42(1):158–170.
- 434 18. Sharif H, Wang L, Wang WL, Magupalli VG, Andreeva L, Qiao Q, et al. Structural
435 mechanism for NEK7-licensed activation of NLRP3 inflammasome. *Nature.* 2019 Jun
436 12;570(7761):338–343.
- 437 19. Spalinger MR, Kasper S, Gottier C, Lang S, Atrott K, Vavricka SR, et al. NLRP3 tyrosine
438 phosphorylation is controlled by protein tyrosine phosphatase PTPN22. *J Clin Invest.*
439 2016 May 2;126(5):1783–1800.
- 440 20. Spalinger MR, Lang S, Gottier C, Dai X, Rawlings DJ, Chan AC, et al. PTPN22 regulates
441 NLRP3-mediated IL1B secretion in an autophagy-dependent manner. *Autophagy.* 2017
442 Sep 2;13(9):1590–1601.
- 443 21. Levy R, Gérard L, Kuemmerle-Deschner J, Lachmann HJ, Koné-Paut I, Cantarini L, et
444 al. Phenotypic and genotypic characteristics of cryopyrin-associated periodic syndrome: a
445 series of 136 patients from the Eurofever Registry. *Ann Rheum Dis.* 2015
446 Nov;74(11):2043–2049.
- 447 22. Tang J, Xiao Y, Lin G, Guo H, Deng H-X, Tu S, et al. Tyrosine phosphorylation of NLRP3
448 by the Src family kinase Lyn suppresses the activity of the NLRP3 inflammasome. *Sci*
449 *Signal.* 2021 Oct 26;14(706):eabc3410.
- 450 23. Nakanishi H, Kawashima Y, Kurima K, Chae JJ, Ross AM, Pinto-Patarroyo G, et al.
451 NLRP3 mutation and cochlear autoinflammation cause syndromic and nonsyndromic
452 hearing loss DFNA34 responsive to anakinra therapy. *Proc Natl Acad Sci USA.* 2017 Sep
453 12;114(37):E7766–E7775.
- 454 24. Rowczenio DM, Pathak S, Arostegui JI, Mensa-Vilaro A, Omoyinmi E, Brogan P, et al.
455 Molecular genetic investigation, clinical features, and response to treatment in 21 patients
456 with Schnitzler syndrome. *Blood.* 2018 Mar 1;131(9):974–981.
- 457 25. Phillips JC, Braun R, Wang W, Gumbart J, Tajkhorshid E, Villa E, et al. Scalable
458 molecular dynamics with NAMD. *J Comput Chem.* 2005 Dec;26(16):1781–1802.

459

460

461 **Tables**

462 **Table 1** : Clinical features of CAPS patients associated with non LRR pathogenic variants and bearing Y861H or
 463 Y861C variants

General features	Non LRR mutated CAPS (n = 48)	LRR mutated CAPS (n = 14)	P-value
Mean age at symptoms onset and range (years old)	4,5 (0-46)	10,1 (3-32)	<0,0001
Mean age at diagnosis and range (years old)	33,7 (0-73)	32,6 (7-54)	0,9015
Mean diagnostic delay and range (years)	29,2 (0-73)	22,4 (4-39)	0,3842
Familial form	35/48 (73%)	14/14 (100%)	0,0290
Mosaicism	4/48 (8%)	0/14 (0%)	0,5659
Clinical features			
Sensorineural hearing loss	29/46 (63%)	14/14 (100%)	0,0060
Urticarial rash	45/48 (94%)	4/14 (29%)	<0,0001
Aphthosis	23/43 (53%)	1/14 (7%)	0,0039
Hypereosinophilia before treatment	0/26 (0%)	3/14 (21%)	0,0368
Headache	21/46 (45%)	12/14 (86%)	0,0128
Meningitis and/or intracerebral hypertension	12/46 (26%)	6/14 (43%)	0,3188
Intellectual impairment	4/47 (9%)	0/14 (0%)	0,5650
Arthromyalgia	42/46 (91%)	11/14 (79%)	0,3375
Conjunctivitis	29/47 (62%)	11/14 (79%)	0,3421
Uveitis and/or papillary edema	18/46 (39%)	7/14 (50%)	0,5434
IBD-like symptoms	4/45 (9%)	1/12 (8%)	>0,9999
Other digestive involvement (abdominal pain, nausea, hepatosplenomegaly)	4/21 (19%)	4/10 (40%)	0,3809
Presence of amyloidosis AA	3/47 (6%)	0/14 (0%)	>0,9999
Mean age at amyloidosis diagnosis and range (years old)	26 (14-38)	/	
Treatment			
Mean age at start of treatment and range (years old)	35,4 (4-74)	34,5 (14-54)	0,9739
Use of anakinra	20/25 (80%)	7/11 (63%)	0,4088
Use of canakinumab	33/33 (100%)	10/10 (100%)	>0,9999
Good response to treatment	41/45 (91%)	14/14 (100%)	0,5635

464 CAPS: cryopyrin-associated periodic syndrome, LRR: leucine-rich-repeat, IBD: inflammatory
 465 bowel disease

466

467

468 **Figure 1: Mutations of residue 861 of NLRP3 drive an inflammasomopathy.**

469 A) Representation of NLRP3 with known mutated amino acid in CAPS patients highlighted in red and
 470 the Y861 in light blue. B) Picture of P6 left eye showing conjunctivitis C) Fundus color photograph of
 471 patient P1 right eye showing an optic disc atrophy. D) Finger of P1 showing digital clubbing fingers. E)
 472 Audiograms of P1. F) Quantification of ASC speck in the plasma of healthy donors, typical CAPS
 473 patients, NLRP3 Y861C patients and FMF patients. G) Quantification of IL-18 in the plasma of healthy
 474 donors and NLRP3 Y861C patients
 475

476 **Figure 2: Pedigrees of 4 families with NLRP3 Y861C and Y861H pathogenic variants.**

477

478 **Figure 3: Cells from patients with Y861C substitution required a boost signal to be activated.**

479 A) Quantification of basal production of IL1 β during overnight culture from PBMC or B) monocytes of
 480 healthy donors, typical CAPS patients and NLRP3 Y861C patients. C) quantification of IL1 β production
 481 of PBMC or D) monocytes of healthy donors, typical CAPS patients and NLRP3 Y861C patients
 482 following LPS and LPS + MSU stimulation (3 hours priming + 3 hours activating signal)
 483

484 **Figure 4: Cells from patients with Y861C substitution demonstrate sustained IL-1 β production.**

485 A) Up: Structure of the NLRP3 (yellow)/NEK7 (red) interface (PDB: 6NPY) near the residue Y861
 486 (cyan). Basic residues of NEK7 (ie K128, K130, R131) are involved in electrostatic interactions (dashed
 487 bond) with W776, E802 and E864 of NLRP3. Down: Predicted impact of selected mutation on
 488 NEK7/NLRP3 interactions through MD simulations. The table display the key interface residues
 489 involved in electrostatic interactions and energies calculations. The interfacial interaction energy is
 490 considered in van der Waals and electrostatic terms. B) As for the previously describe R920Q mutation,
 491 Y861C is predicted to stabilize NLRP3/NEK7 interaction compared to WT. However, Y861H is
 492 predicted to be detrimental B) Quantification of IL1 β production over time of monocytes from healthy
 493 donors and 3 NLRP3 Y861C patients. C) Quantification of the production of IL1 β between 3 hours and
 494 6 hours post boost in monocytes healthy donors and NLRP3 Y861C patients.
 495

496 **Figure 5: Graphical abstract.** CAPS patients with pathogenic variant at position 861 of NLRP3 are
 497 more susceptible to headache and hearing loss than patients with variants in the NACHT domain.
 498 Inversely, NACHT mutated patients are more susceptible to aphthosis and urticarial rash.

Figure 1

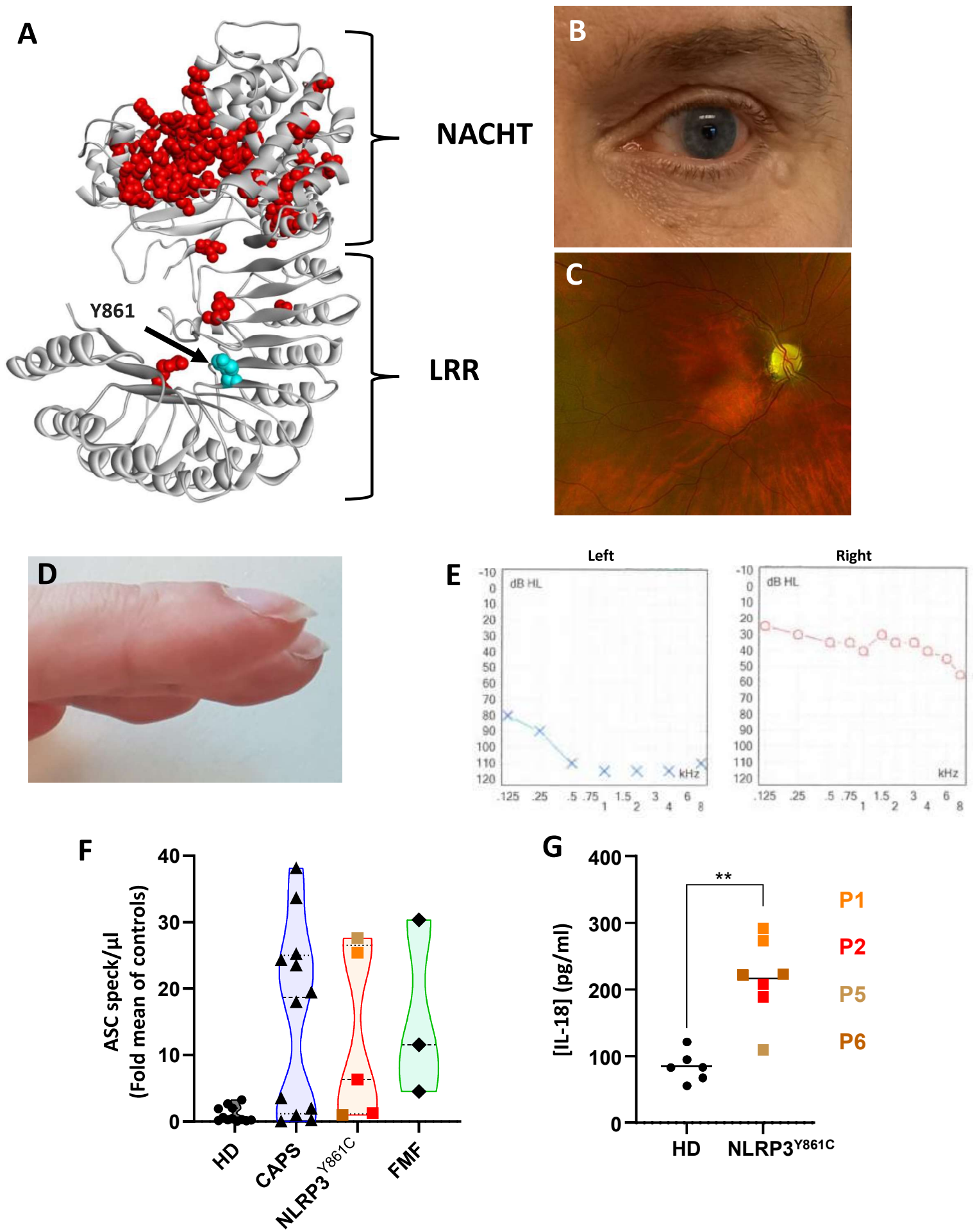
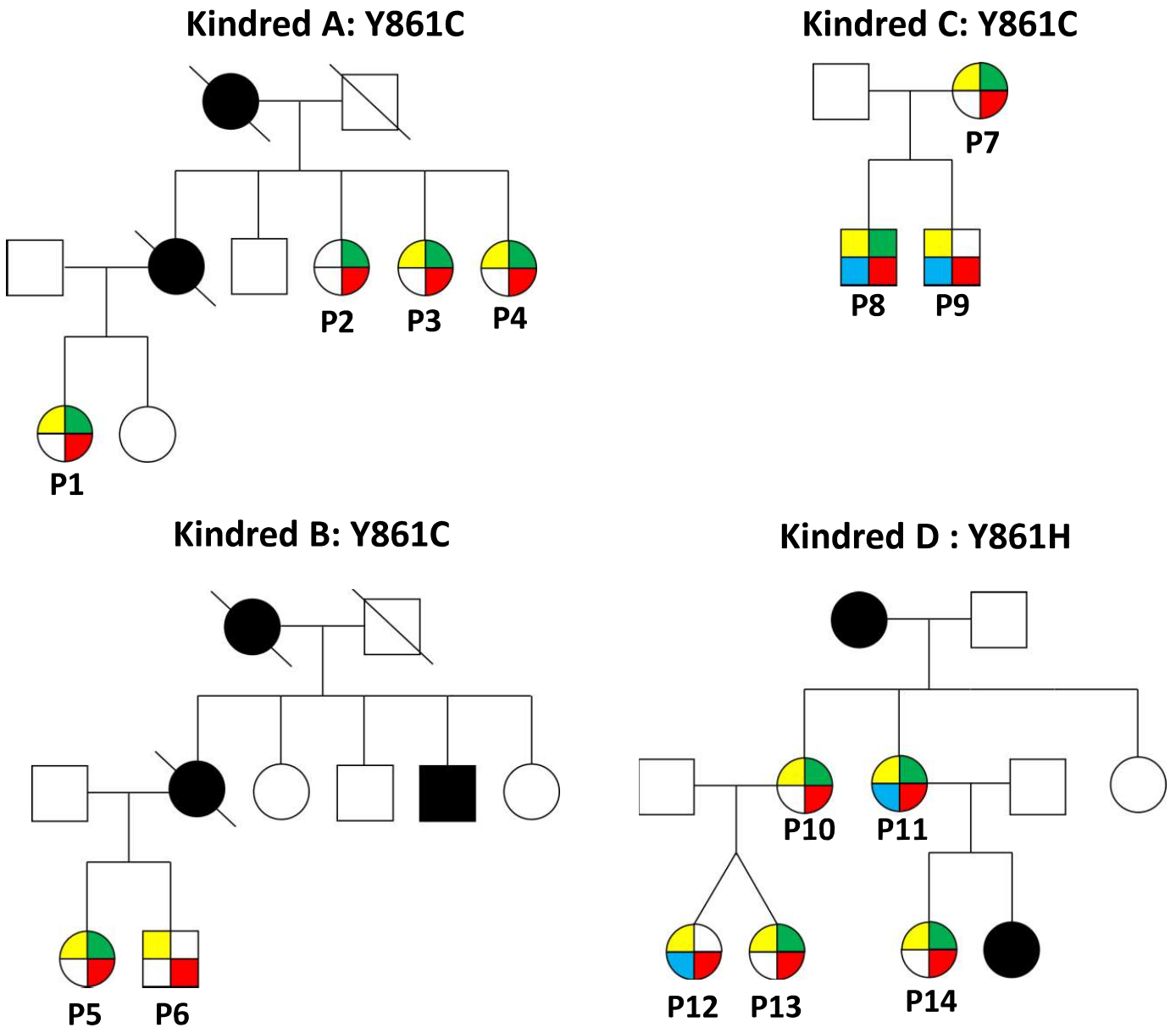


Figure 2



- Sensorineural hearing loss
- Urticarial rash
- Arthromyalgia
- Ocular involvement

- Individual without CAPS related symptoms
- Individual with CAPS related symptoms not assessed

Figure 3

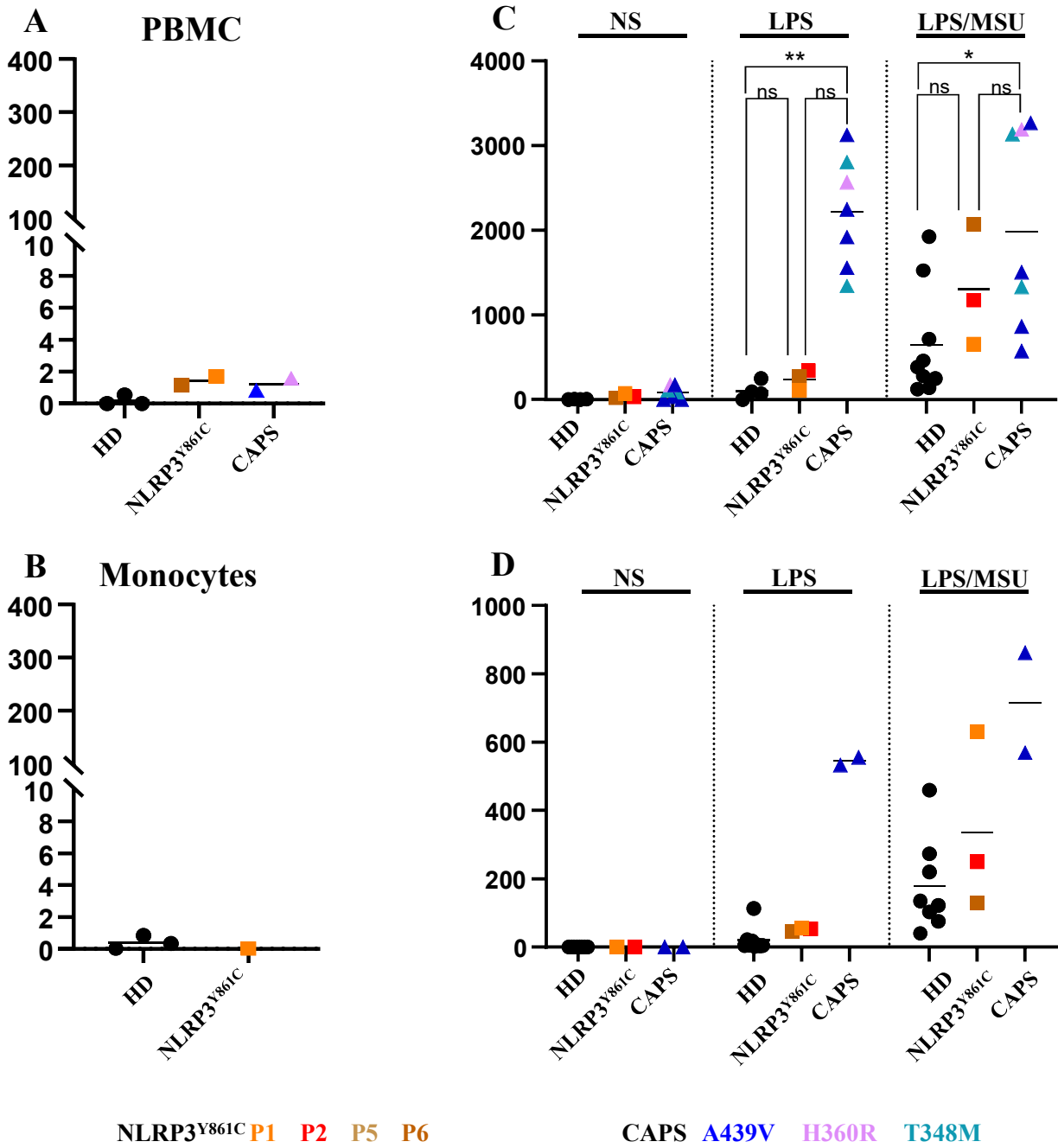
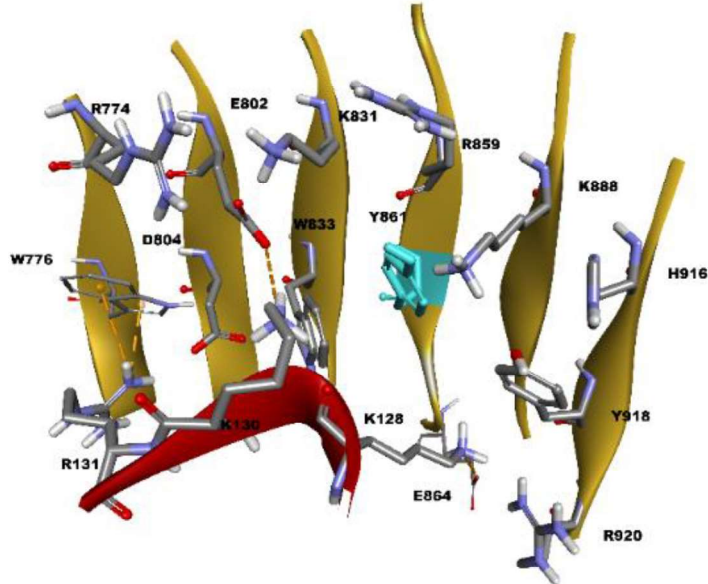


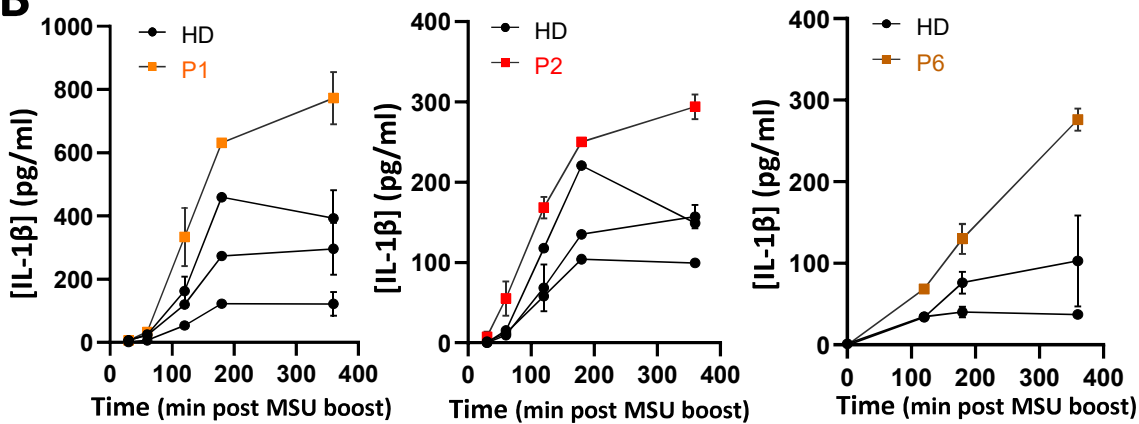
Figure 4

A



NLRP3 Genotypes	Interacting AA from NLRP3	Interacting AA from NEK7	Interaction energy (kcal/mol)	Electrostatic energy (kcal/mol)	Van der Waals energy (kcal/mol)
Y861 (WT)	D750, D804, D807, E864	R121, K128, R131, K140	-383.0	-326.9	-56.1
C861	E356, K696, D747, D750	R131, K140, D261, R294	-501.9	-424.2	-77.7
H861	K696, D750, E864	K128, K140, D261	-351.2	-310.1	-41.1
Q920	K696, D750, D804, E864, E1007, E1033,	K124, K127, K128, R131, K140, D261	-451.8	-413.0	-38.8

B



C

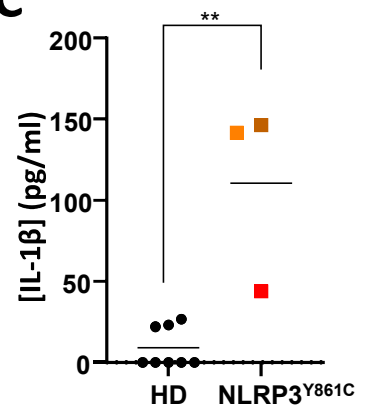
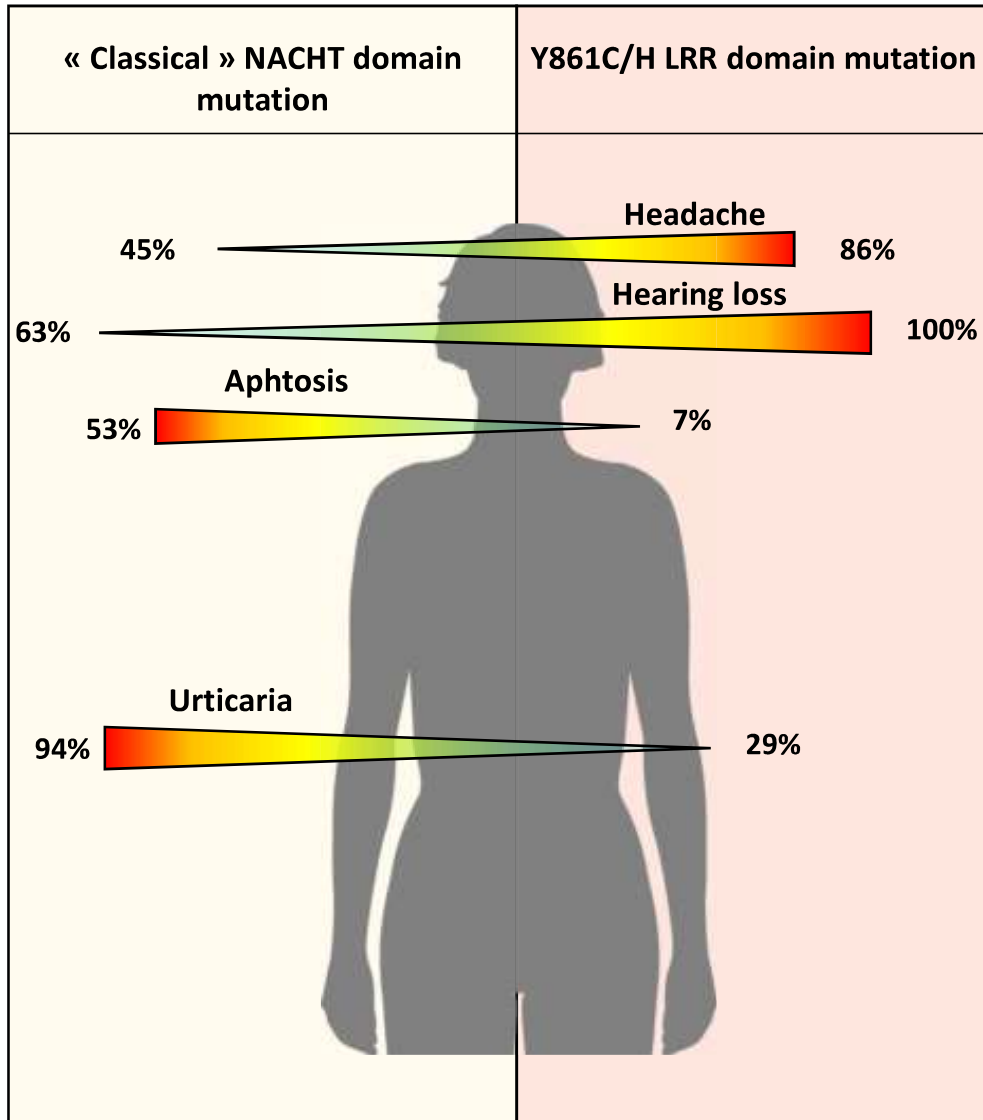
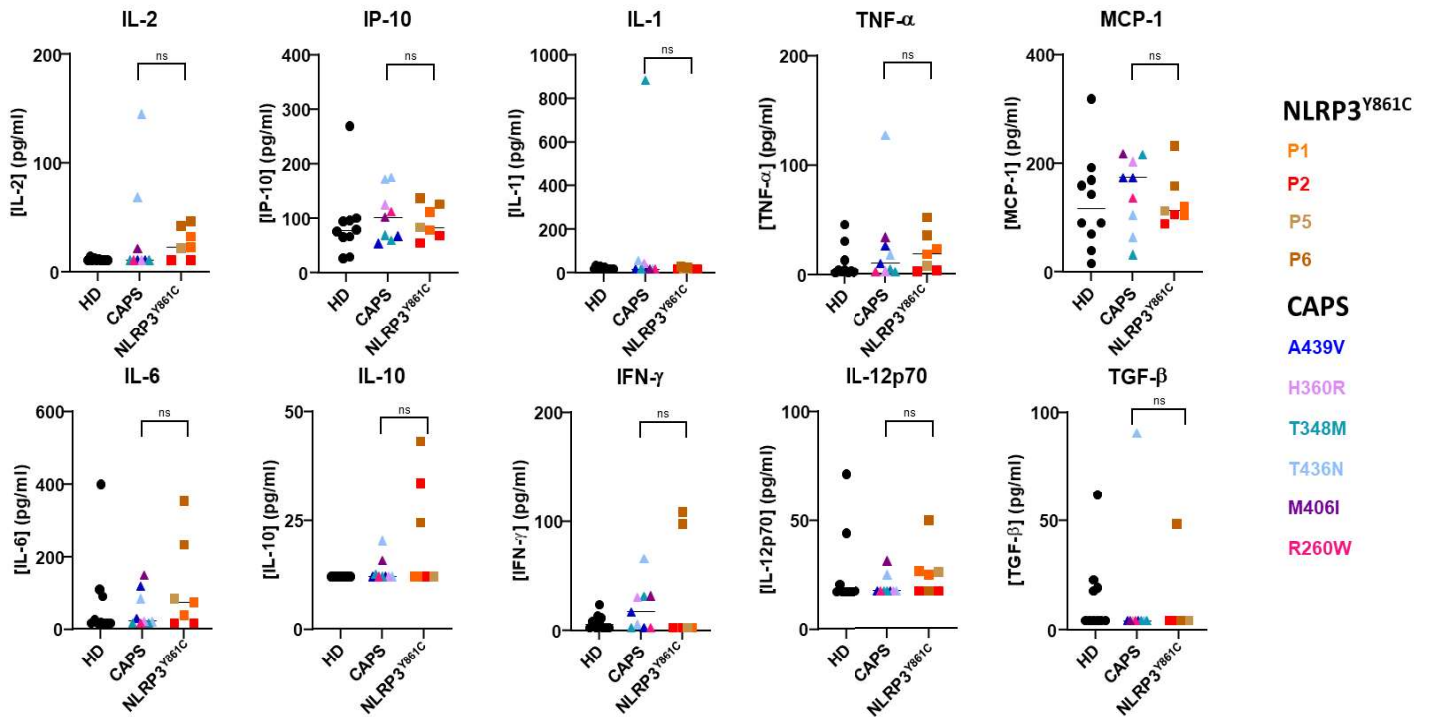


Figure 5



Sup Fig 1



Sup fig 1: Screening of the plasmatic levels of 10 inflammatory cytokines did not reveal any significant difference between typical CAPS and NLRP3 Y861C patients.